5706–5716 *Nucleic Acids Research, 2007, Vol. 35, No. 17* *Published online 22 August 2007*
doi:10.1093/nar/gkm500

Physical and functional interactions between Werner syndrome helicase and mismatch-repair initiation factors

Nurten Saydam[1] Radhakrishnan Kanagaraj[1], Tobias Dietschy[1,2,3], Patrick L. Garcia[1], Javier Peña-Diaz[1], Igor Shevelev[2,3], Igor Stagljar[2,3] and Pavel Janscak[1,*]

[1]Institute of Molecular Cancer Research of the University of Zurich, Switzerland, [2]Department of Biochemistry and [3]Department of Medical Genetics and Microbiology, Donnelly Centre for Cellular and Biomolecular Research, University of Toronto, Canada

Received April 26, 2007; Revised and Accepted June 7, 2007

ABSTRACT

Werner syndrome (WS) is a severe recessive disorder characterized by premature aging, cancer predisposition and genomic instability. The gene mutated in WS encodes a bi-functional enzyme called WRN that acts as a RecQ-type DNA helicase and a 3′-5′ exonuclease, but its exact role in DNA metabolism is poorly understood. Here we show that WRN physically interacts with the MSH2/MSH6 (MutSα), MSH2/MSH3 (MutSβ) and MLH1/PMS2 (MutLα) heterodimers that are involved in the initiation of mismatch repair (MMR) and the rejection of homeologous recombination. MutSα and MutSβ can strongly stimulate the helicase activity of WRN specifically on forked DNA structures with a 3′-single-stranded arm. The stimulatory effect of MutSα on WRN-mediated unwinding is enhanced by a G/T mismatch in the DNA duplex ahead of the fork. The MutLα protein known to bind to the MutSα–heteroduplex complexes has no effect on WRN-mediated DNA unwinding stimulated by MutSα, nor does it affect DNA unwinding by WRN alone. Our data are consistent with results of genetic experiments in yeast suggesting that MMR factors act in conjunction with a RecQ-type helicase to reject recombination between divergent sequences.

INTRODUCTION

Werner syndrome (WS) is an autosomal recessive disorder characterized by an early onset of age-related pathologies including graying hair, alopecia, arteriosclerosis, osteoporosis, diabetes mellitus and cancer (1). The gene mutated in WS, *WRN*, encodes a RecQ-type DNA helicase (2,3). WRN also possesses a 3′ - 5′ exonuclease activity residing in a separate domain located at the N-terminus of the protein (4,5). At the cellular level, WRN deficiency is associated with defects in DNA replication, homologous recombination (HR) and telomere maintenance (6–9). As a result, cells derived from WS patients display a high degree of genomic instability including elevated levels of chromosomal translocations and deletions (10–13). WS cells are hypersensitive to DNA-damaging agents such as 4-nitroquinoline 1-oxide, topoisomerase inhibitors and DNA cross-linkers, suggesting that WRN is actively involved in DNA repair (14–16). Several lines of evidence implicate WRN in the cellular response to DNA double-strand breaks (DSBs). WRN is rapidly recruited to the sites of ionizing radiation (IR)-induced damage (17). Moreover, it interacts physically and functionally with a number of proteins that are involved in the DSB-repair process including the MRE11-RAD50-NBS1 (MRN) complex (18), the Ku complex (19), RAD52 (20) and DNA-dependent protein kinase (21). However, the precise role for WRN in DNA repair remains to be elucidated.

The DNA mismatch-repair (MMR) system maintains genomic integrity by correcting DNA replication errors and preventing recombination between divergent sequences (22,23). Defects in a subset of MMR genes including *MSH2*, *MSH3*, *MSH6*, *MLH1* and *PMS2* are associated with hereditary non-polyposis colon cancer, highlighting the crucial role for MMR in genome maintenance (24). In the initiation step of the eukaryotic

*To whom correspondence should be addressed. Tel: +41(0)44 635 3470; Fax: +41(0)44 635 3484; Email: pjanscak@imcr.unizh.ch
Present address:
Nurten Saydam, Harvard School of Public Health, 667, Huntington Ave, Boston, USA.

The authors wish it to be known that, in their opinion, the first three authors should be regarded as joint First Authors.

MMR process, at least three heterodimers, namely MSH2/MSH6 (MutSα), MSH2/MSH3 (MutSβ) and MLH1/PMS2 (MutLα), are involved (22). MutSα binds to base-base mismatches and short insertion/deletion loops, while MutSβ can recognize only insertion/deletion loops containing up to 16 extra nucleotides in one strand (22). MutLα possesses an intrinsic endonuclease activity, which is activated upon mismatch recognition and introduces incisions in the discontinuous strand of the heteroduplex DNA, generating entry sites for the 5′-3′ exonuclease EXO1 (25).

Sgs1, the yeast ortholog of WRN, also contributes to the suppression of recombination between divergent DNA sequences (26). Heteroduplex rejection during repair of DSBs by the single-strand annealing pathway of HR in yeast requires the mismatch binding and ATPase functions of the Msh2p/Msh6p heterodimer and the helicase activity of Sgs1 (27,28). These findings led to the proposal that MMR proteins act in conjunction with Sgs1 to unwind DNA recombination intermediates containing mismatches (27,28).

Here we demonstrate that WRN directly interacts with MutSα, MutSβ and MutLα via distinct domains. MutSα and MutSβ are found to stimulate WRN-mediated unwinding of forked DNA duplexes with a 3′-single-stranded (ss) arm. The stimulatory effect of MutSα on WRN-mediated unwinding is enhanced by a single G/T mismatch located in the duplex ahead of the fork in a manner independent of MutLα. These data provide biochemical evidence suggesting that the rejection of homeologous recombination by MMR proteins occurs *via* helicase-mediated unwinding of recombination intermediates.

MATERIALS AND METHODS

Construction of plasmids

The bacterial expression vectors for the WRN fragments encompassing the amino acid residues 51–449, 949–1432, 500–946, 500–1149, 500–1236, respectively, fused to the C-terminus of glutathione *S*-transferase (GST) were constructed by PCR amplification of corresponding regions of the WRN cDNA and their insertion in pGEX-2TK (Amersham Biosciences) between the EcoRI and BamHI sites. The complete coding region of WRN was amplified by PCR and cloned in pACT2 (Clontech Palo Alto, CA) via SmaI site to construct a yeast two-hybrid (YTH) vector expressing WRN as a fusion with a Gal4 activation domain. MLH1 cDNA comprised of the codons 500–756 was cloned in a YTH vector pBTM116 (Clontech Palo Alto, CA) between the EcoRI and SalI sites, resulting in a fusion with a LexA DNA binding domain. The pBTM16 derivatives expressing other MLH1 variants as well as the full-length yMlh1 were previously described (29). The Gal4-hMSH2 (pLJR105), LexA-MSH3 and LexA-MSH6 bait plasmids were also described previously (30,31).

Proteins

Recombinant human WRN (3,32), MutSα (33), MutSβ (33) and MutLα (34) and *Escherichia coli* MutS (35) were produced and purified as previously described. An antibody against the N-terminal region of WRN encompassing amino acids 1–391 (ISEV-391) was raised in rabbit and purified on an antigen-coupled Sepharose 4A column (Amersham Biosciences). Control IgGs were purified from a rabbit preimmune serum on a 5 ml HiTrap protein G-Sepharose column (Amersham Biosciences).

Cell culture

The following human cell lines were used in this study: HEK 293 embryonic kidney cells and AG11395 SV40-transformed WS fibroblasts (Coriell Institute for Medical Research). The HEK 293 cells were maintained in DMEM (Gibco) supplemented with 10% fetal calf serum (Biochrome AG). The WS cells were maintained in MEM containing 15% fetal calf serum and 2 mM L-glutamine.

Immunoprecipitation assays

Cells were suspended in lysis buffer containing 20 mM Tris–HCl (pH 7.5), 150 mM NaCl, 2 mM EDTA, 0.1% (v/v) Triton X-100, 10% (v/v) glycerol and complete, EDTA-free protease inhibitor cocktail (Roche). After sonication, the suspension was centrifuged at 20 000 *g* for 30 min at 4°C. Aliquots containing 1.6 mg of protein were incubated overnight at 4°C with purified rabbit polyclonal anti-WRN IgGs (2 μg), which was followed by a 2-h incubation with protein A/G-agarose beads (Santa Cruz) at 4°C. Where required, extracts were treated with 50 U of DNaseI (Roche) for 30 min at 25°C prior to addition of antibody. After extensive washing with the lysis buffer, the immunoprecipitates were subjected to electrophoresis in a 7.5% polyacrylamide–SDS gel followed by western blotting. The blots were probed with mouse monoclonal antibodies against WRN (BD Biosciences, 611169), MSH6 (Pharmingen, clone 44), PMS2 (Pharmingen, clone 16-4), MLH1 (BD Biosciences, 554073), MSH2 (Calbiochem, clone NA 26) and MSH3 (Transduction Laboratories, clone 52). Immune complexes were detected using ECL-plus reagent (Amersham Biosciences), with horse anti-mouse IgG-horseradish peroxidase conjugate (Vector) used as a secondary antibody. In the control experiment, IgGs purified from a preimmune rabbit serum were used instead of the anti-WRN antibody.

GST pull-down assays

GST–WRN fusion proteins were produced in the *E. coli* BL21-CodonPlus(DE3)-RIL strain (Stratagene) using the expression vectors described above. The fusion proteins were bound to glutathione–sepharose beads (Amersham Biosciences) as previously described (36). The beads were incubated with 1 μg of purified MutSα, MutSβ or MutLα in 400 μl of NET-N 100 buffer [10 mM Tris HCl (pH 8.0), 1 mM EDTA, 100 mM NaCl, 0.5% (v/v) NP-40] for 2 h at 4°C. After extensive washing with NET-N 100 buffer, proteins bound to the beads were analyzed by western blotting. Membranes were probed with the monoclonal antibodies described above. MSH3 was detected with a rabbit polyclonal antibody (NTH3) raised against its first 200 amino acids (Eurogentec). In a control experiment, beads were coated with GST protein only.

ELISA-based protein binding assay

Purified recombinant WRN was diluted to a concentration of 20 nM in carbonate buffer [16 mM Na_2CO_3, 34 mM $NaHCO_3$ (pH 9.6)] and added to wells of a 96-well microtiter plate (50 µl/well). Plates were incubated overnight at 4°C. For control reactions, wells were pre-coated with an equivalent amount of bovine serum albumin (BSA). After aspiration of the samples, the wells were blocked with blocking buffer [phosphate-buffered saline, 0.5% (v/v) Tween-20 and 3% (w/v) BSA] for 2 h at 37°C (200 µl/well). Following blockage, the wells were incubated with increasing concentrations of purified recombinant MutSα, MutSβ and MutLα proteins for 1 h at 37°C. All samples were supplemented with ethidium bromide (EtBr) at a concentration of 50 µg/ml to prevent DNA-mediated interactions. Wells were washed four times with blocking buffer to eliminate unbound proteins, and incubated with the appropriate primary antibody diluted in blocking buffer (mouse monoclonal anti-MSH2 antibody for MutSα and MutSβ, and mouse monoclonal anti-MLH1 antibody for MutLα). Plates were incubated for 1 h at 37°C. After four washings with blocking buffer, horseradish peroxidase-conjugated anti-mouse secondary antibody (1:10 000 in blocking buffer) was added and the plates were incubated at 37°C for 30 min. After extensive washing with blocking buffer, the protein complexes were detected using o-Phenylenediamine dichloride (Sigma) dissolved in 0.1 M citrate-phosphate buffer (pH 5.0) containing 0.03% hydrogen peroxide (1 mg/ml). The reactions were terminated after 5 min by adding 50 µl of 2 M H_2SO_4. The plates were scanned in a microplate reader (Molecular Devices) for absorbance at 492 nm. The A_{492} values, corrected for background signal in the presence of BSA, were plotted as a function of the concentration of appropriate MMR protein using the GraphPad Prism software. To determine an apparent dissociation constant of each complex (K_d), the data points were fitted by the hyperbolic function $Y = B_{max} * X/(K_d + X)$ where B_{max} is the maximal binding and K_d is the concentration of ligand required to reach half-maximal binding.

YTH assay

YTH analysis was carried out using *Saccharomyces cerevisiae* strains L40 (*MAT*a t*rp1 leu2 his3 LYS2::lexA-HIS3 URA3::lexA-lacZ*) and Y190 (*MATα*, *ura3-52, his3-200*, *lys2-801, ade2-101, trp1-901, leu2-3, 112, gal4Δ*, *gal80Δ*, *cyh*^{r}*2, LYS2::GAL1*$_{UAS}$*-HIS3*$_{TATA}$*-HIS3, URA3::GAL1*$_{UAS}$*-GAL1*$_{TATA}$*-lacZ*). The former strain was used for LexA-bait vectors while the latter strain was used for Gal4-bait vectors. Clones carrying the bait and prey plasmids were tested for β-galactosidase activity using a pellet X-gal (PXG) assay as previously described (37).

Helicase assays

Schemes of DNA substrates as well as the sequences of the constituent oligonucleotides are summarized in Supplementary Table 1. The f11-20 oligonucleotide (50-mer) was labeled at the 5′-end using T4 polynucleotide kinase (NEB) and [γ-^{32}P]ATP (Amersham Biosciences), and annealed with appropriate oligonucleotides under previously described conditions (38). The helicase reaction mixtures (10 µl) contained 50 mM Tris–HCl (pH 7.5), 50 mM NaCl, 2 mM $MgCl_2$, 50 µg/ml of BSA, 2 mM ATP, 1 mM DTT, 1 nM DNA substrate and indicated concentrations of MMR proteins (MutSα, MutSβ, MutLα and MutS) and WRN. The MMR proteins were pre-incubated with the DNA substrate on ice for 1 min prior to the addition of WRN. The reactions were incubated at 37°C for 30 min and terminated by the addition of 0.5 reaction volume of buffer S [150 mM EDTA, 2% (w/v) SDS, 30% (v/v) glycerol, 0.1% (w/v) bromophenol blue] followed by treatment with proteinase K (0.1 mg/ml) at 37°C for 10 min. The reaction products were resolved on a non-denaturing 10% polyacrylamide gel [acrylamide to bis-acrylamide, 19:1 (w/w)] run in 1xTBE buffer at 140 V. Radiolabeled DNA species were visualized by a phosphorimager and quantified using ImageQuant software (Molecular Dynamics).

RESULTS

Physical association between WRN and MMR proteins

Based on genetic studies in yeast, it has been suggested that the proteins involved in the initiation of MMR act in conjunction with RecQ DNA helicases to eliminate DNA recombination intermediates containing mismatches, which can give rise to chromosomal rearrangements (27,28). We sought to test the validity of this model biochemically using the WRN helicase, one of the five RecQ homologs identified in human cells, whose dysfunction results in chromosomal translocations and deletions. First, we performed an ELISA-based protein-binding assay to investigate whether WRN and the MMR proteins interact physically. Increasing concentrations of purified MutSα (MSH2/MSH6), MutSβ (MSH2/MSH3) and MutLα (MLH1/PMS2) proteins (Figure 1A) ranging from 0 to 80 nM were incubated in wells that had been pre-coated with WRN at a concentration of 20 nM and subsequently blocked with BSA to prevent non-specific interactions. After extensive washing, the bound MMR proteins were incubated with specific antibodies followed by a colorimetric assay to quantify the binding. In control experiments, MMR proteins were incubated in wells pre-coated only with BSA. We found that all the three MMR heterodimers were specifically bound to WRN-coated wells in a dose dependent manner, indicating a direct interaction (Figure 1B–D). Interestingly, the apparent dissociation constant of the MutSβ–WRN complex (K_d = 8.8 nM) was much lower than that estimated for the MutSα–WRN complex (K_d = 38.5 nM). The dissociation constant of the MutLα–WRN complex (K_d = 34.9 nM) was similar to that of the MutSα–WRN complex.

To test whether WRN and MMR proteins form a stable complex *in vivo*, we immunoprecipitated WRN from extracts of exponentially growing human embryonic kidney cells (HEK 293) and subjected the resulting immunoprecipitate to western blot analysis.

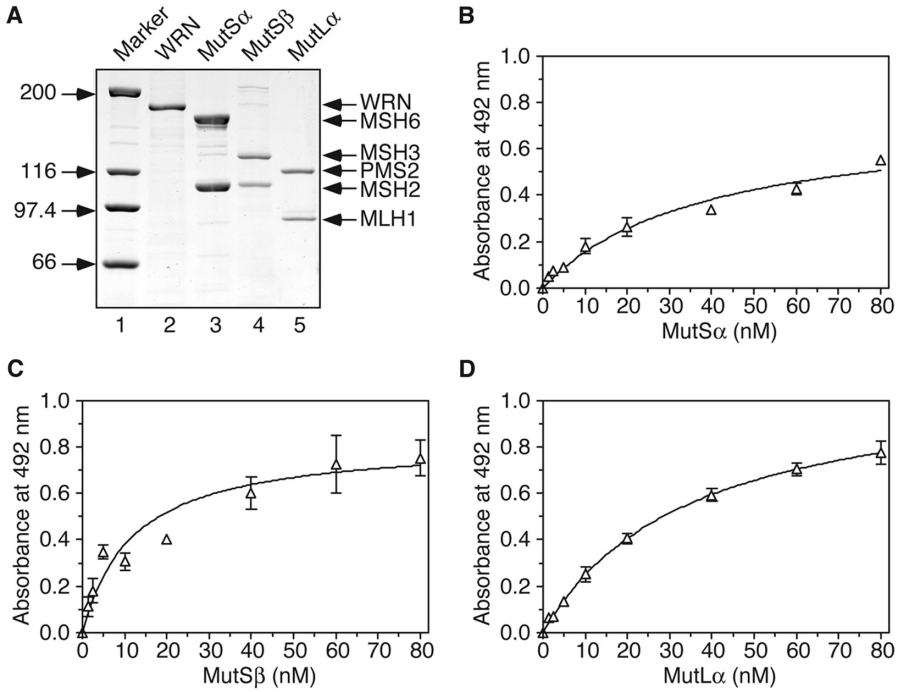

Figure 1. Direct physical interaction of WRN with MMR proteins. (**A**) SDS–PAGE analysis of purified recombinant MutSα, MutSβ, MutLα and WRN proteins produced in insect cells by means of the baculovirus system. (**B**) Binding of MutSα to WRN as a function of MutSα concentration. (**C**) Binding of MutSβ to WRN as a function of MutSβ concentration. (**D**) Binding of MutLα to WRN as a function of MutLα concentration. Increasing concentrations of MutSα, MutSβ and MutLα (0–80 nM) were incubated at 37°C for 1 h in the wells of an ELISA plate that were pre-coated with the WRN protein (20 nM) and subsequently blocked with 3% BSA. After extensive washing, the bound MMR proteins were detected by ELISA as described in Materials and Methods. The measured absorbance values were corrected by subtracting background values obtained with BSA-coated wells. The data points represent the mean of three independent experiments.

This immunoprecipitate was found to contain the MLH1 and PMS2 proteins, components of the MutLα complex, but not the MSH2 and MSH6 proteins, which form the MutSα heterodimer (Figure 2A, lanes 3 and 4). None of these MMR proteins were detected in the immunoprecipitate obtained with control IgGs (Figure 2A, lane 2). To exclude the possibility that the observed association of WRN with MLH1 and PMS2 results from independent binding of these proteins to DNA, we pre-treated the cell extracts with DNaseI. We found that this treatment did not alter the level of the MMR proteins in the WRN immunoprecipitate, suggesting that the WRN–MLH1–PMS2 complex is mediated by protein–protein interactions (Figure 2A, compare lanes 3 and 4). Furthermore, we did not detect PMS2 in an immunoprecipitate obtained with anti-WRN antibody from extracts of the WS cell line AG11395, excluding the possibility that the observed co-immunoprecipitation of MMR proteins with WRN is due to cross-reactivity of the antibody (Figure 2B).

Collectively, these data indicate that MutLα but not MutSα, forms a stable complex with WRN *in vivo*.

Mapping of protein–protein interaction domains

To identify the MutSα, MutSβ and MutLα-interaction sites on WRN, we performed affinity pull-down assays using a series of WRN fragments fused to GST. These fragments covered the entire WRN polypeptide except for the first 50 amino acids and the region spanning the amino acids 450–499 (Figure 3A and B). The GST pull-down experiments revealed that the MutSα interaction site on WRN was localized to the region between amino acids 500 and 946, which constitutes the helicase core of WRN composed of the DExH helicase and Zn-binding domains (Figure 3A and C). MutSβ was found to make contacts not only with the helicase core of WRN, but also with a region spanning amino acids 947–1149 that contains the winged-helix (WH) motif, a common interaction site for most of the WRN partners identified thus far (Figure 3A and C) (39). Notably, the binding affinity of MutSβ to the WH domain of WRN appeared to be much higher that its binding affinity to the helicase core of WRN (Figure 3C, compare lanes 4–7). The data also indicated that MutSβ binds to WRN more efficiently than MutSα (Figure 3C, top and middle panels; compare lane 1 with lanes 4–7), which is in agreement with the results of the ELISA assay (Figure 1).

MutLα was found to interact with the helicase core of WRN and with the N-terminal portion of WRN including the exonuclease domain, showing a higher binding affinity to the former domain (Figure 3A and C, bottom panel; compare lanes 3–7).

To identify the subunits of MutSα, MutSβ and MutLα that mediate the interaction with WRN, we performed a quantitative YTHassay with the full-length WRN as prey. The following interactions were examined: MSH2–WRN, MSH6–WRN, MSH3–WRN and MLH1–WRN.

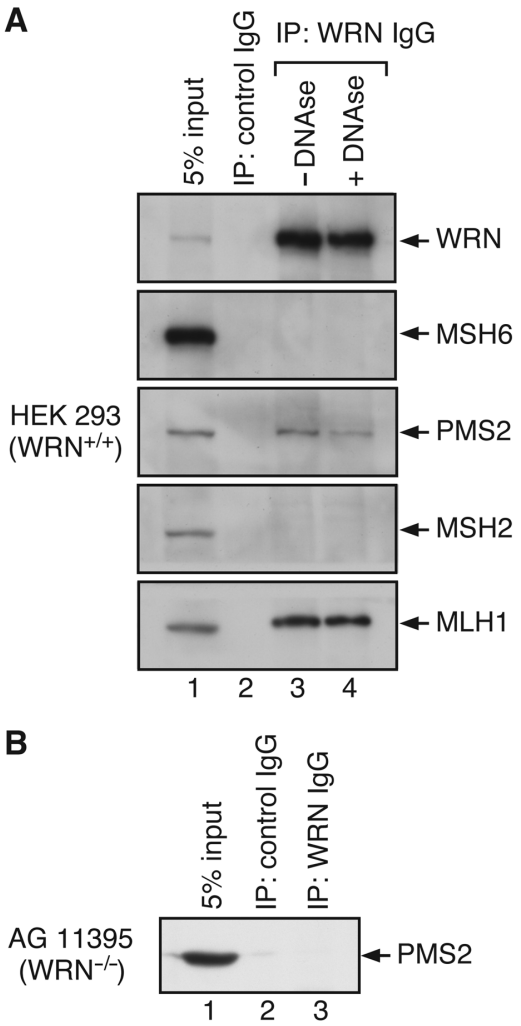

Figure 2. WRN forms a stable complex with MLH1 and PMS2 in human cells. (**A**) Western blot analysis of WRN immunoprecipitates from total extracts of HEK 293 cells (1.6 mg of protein) before (lane 3) and after (lane 4) treatment with DNaseI (50 U). Lane 1, 5% of input; lane 2, control immunoprecipitation experiment with a preimmune rabbit IgGs. Purified rabbit anti-WRN IgGs (2 μg) were used to immunoprecipitate WRN. Blots were probed with monoclonal antibodies against WRN, MSH2, MSH6, MLH1 and PMS2. (**B**) Western blot analysis of immunoprecipitate from extracts of AG11395 ($WRN^{-/-}$) cells obtained using an anti-WRN antibody. The immunoprecipitations were carried out under the same conditions as in (A). The blots were probed with a monoclonal antibody against PMS2.

We found WRN to interact with MLH1 and MSH2, but not with MSH3 and MSH6 (Figure 4A and B). This indicates that the MutSα–WRN and MutSβ–WRN interactions are mediated by MSH2, and the MutLα–WRN interaction is mediated by MLH1. However, the inability of MSH3 and MSH6 to interact with WRN in the YTH assay could be a consequence of the fact that these proteins are not soluble when expressed alone (33). This is also true for PMS2 (34). Therefore, the possibility still exists that these proteins could make additional contacts with WRN. This is particularly likely in the case of MSH3, since our GST pull-down experiments revealed that MutSβ interacts with both the helicase core and the WH domain of WRN, whereas MutSα interacts only with the helicase core of WRN (Figure 3).

In order to identify the WRN interaction domain on MLH1, we tested a series of MLH1 deletion variants for the ability to interact with the full-length WRN in YTH assay. We found that this domain is located at the C-terminus of the MLH1 polypeptide between amino acids 500 and 756 (Figure 4A and B). This is different from the location of the BLM-interaction site that was mapped to the region spanning amino acids 396–500 (29).

Stimulation of the helicase activity of WRN by MutSα and MutSβ

Next, we tested MutSα for the ability to affect the helicase activity of WRN on DNA substrates containing mismatches. In these experiments, we used a synthetic DNA duplex (49 bp) with a 3′-ss flap (19 nt) resembling a part of the structure that results from annealing of the resected arms of a broken chromosome at regions of homology. On such forked DNA structures, WRN preferentially translocates along the 3′-flap oligonucleotide to unwind the duplex ahead of the fork junction, generating a 3′-tailed duplex. This primary product can be further unwound by WRN into the component strands, as a consequence of loading of a second helicase molecule on the 3′-ssDNA tail (40). We prepared a fully matched substrate and a substrate containing a single G/T mismatch located 11 nt ahead of the ss/ds junction (Figure 5A and B, top panels). WRN alone displayed a very low helicase activity on both structures when present at the same concentration as the DNA substrate (1 nM). However, the helicase activity of WRN on these structures dramatically increased upon inclusion of an 8-fold molar excess of MutSα in the reaction (Figure 5A–D). Notably, the initial rate of the MutSα-stimulated unwinding reaction with G/T substrate was about 1.7 times higher than that measured with the G/C substrate (Supplementary Table 2).

Since MutLα is known to bind to MutSα–heteroduplex complexes (41), we investigated whether it can affect the WRN-mediated unwinding of G/T and G/C substrates induced by MutSα. We found that MutLα did not significantly alter the MutSα-dependent helicase activity of WRN on these DNA structures (Figure 5). Also, it had no effect on WRN-mediated unwinding in the absence of MutSα (Figure 7, lane 5).

To further assess the effect of MutSα on WRN-mediated unwinding of the 3′-flap duplex, we performed a protein titration experiment, in which we varied the concentration of MutSα while keeping WRN and DNA substrate at a fixed concentration of 1 nM. We found that MutSα stimulated the helicase activity of WRN in a concentration-dependent manner, exhibiting a significantly higher activity on the G/T substrate than on the homoduplex substrate (Figure 6).

To explore the specificity of the observed stimulatory effect, we tested human MutSβ as well as *E. coli* MutS for the ability to stimulate DNA unwinding by WRN. We found that MutSβ enhanced the WRN-mediated unwinding of the 3′-flap DNA duplex to a similar extent

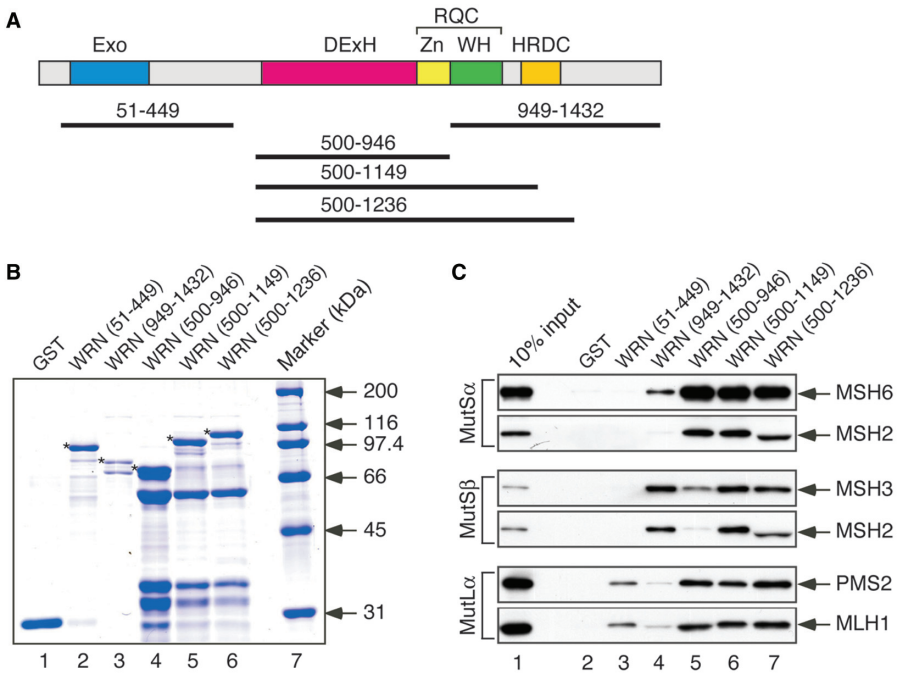

Figure 3. Mapping of MutSα, MutSβ and MutLα-interaction domains on WRN (**A**) Domain organization of the WRN protein. Exo, exonuclease domain; DExH, helicase domain; Zn, zinc-binding domain; WH, winged-helix domain; HRDC, helicase and RNaseD C-terminal domain; RQC, RecQ C-terminal region. The black lines indicate the boundaries of the various WRN fragments used in this study. (**B**) SDS–PAGE analysis of GST–WRN fragments expressed in *E. coli* and isolated using glutathione beads. Bands migrating below the WRN fragments (marked by an asterisks) were determined to be degradation products by western blot analysis using an anti-GST antibody. (**C**) GST pull-down assay. Glutathione beads coated with the indicated GST-tagged WRN fragments were incubated with purified MutSα, MutSβ or MutLα proteins expressed in insect cells using baculovirus system and the bound MMR proteins were analyzed by western blotting as described in Materials and Methods.

as seen with MutSα (Figure 7, compare lanes 2 and 3). In contrast, the *E. coli* MutS protein did not enhance the WRN-mediated DNA unwinding (Figure 7, lane 8), indicating that the observed stimulatory effect is specific to human MutS homologs. As in the case of MutSα, MutSβ-stimulated helicase activity of WRN was not influenced upon addition of MutLα (Figure 7, compare lanes 4 and 7) and it was dependent on MutSβ concentration (Supplementary Figure S1). We also found that in the presence of MutSβ, WRN unwound the G/T substrate with the same efficiency as the homoduplex substrate (Supplementary Figure S2). This is consistent with the fact that MutSβ does not bind to base–base mismatches (22) and supports the conclusion that the observed stimulatory effect of the G/T mismatch on MutSα-dependent unwinding of the 3′-flap duplex by WRN results from the specific binding of MutSα to the mismatch.

Together, the results described above indicate that MutSα and MutSβ, but not MutLα, can stimulate WRN to unwind DNA structures resembling recombination intermediates and that this stimulatory effect is enhanced by mismatches in the DNA substrate.

MutSα and MutSβ stimulate WRN helicase specifically on forked DNA duplexes with a 3′-ss arm

To gain further insights into the mechanism underlying the stimulation of the helicase activity of WRN by MutSα and MutSβ, we investigated the dependence of this reaction on the configuration of the arms of the fork. Using the same set of oligonucleotides, we prepared the following substrates: a forked duplex with both arms single stranded (splayed arm); a forked duplex with the 3′-arm single stranded and the 5′-arm double stranded (3′-flap duplex); a forked duplex with the 3′-arm double stranded and the 5′-arm single stranded (5′-flap duplex) and a forked duplex with both arms double stranded. Earlier studies revealed that WRN could unwind efficiently all these structures, indicating that it does not require the 3′-arm to be single stranded for loading at the fork (40). We found that MutSα and MutSβ strongly stimulated the WRN-mediated unwinding of the splayed arm and the 3′-flap duplex, but had no significant effect on the unwinding of the 5′-flap duplex and the fully double stranded fork (Figure 8). We also tested these proteins for the ability to stimulate the helicase activity of WRN on 3′-ssDNA-tailed duplex, which is normally a poor substrate for WRN (40). We found that neither MutSα nor MutSβ could activate WRN for unwinding of this partial DNA duplex (data not shown). Interestingly, the 3′-tail duplex resulting from unwinding of the 3′-flap structure was unwound by WRN efficiently. This discrepancy can result from the fact that WRN exists as an oligomeric structure, which would facilitate loading of a second molecule of WRN on the 3′-ssDNA generated by unwinding of the duplex ahead of the fork.

Collectively, these data indicate that MutSα and MutSβ require a forked DNA structure with 3′-ss DNA at the junction to stimulate WRN-mediated DNA unwinding.

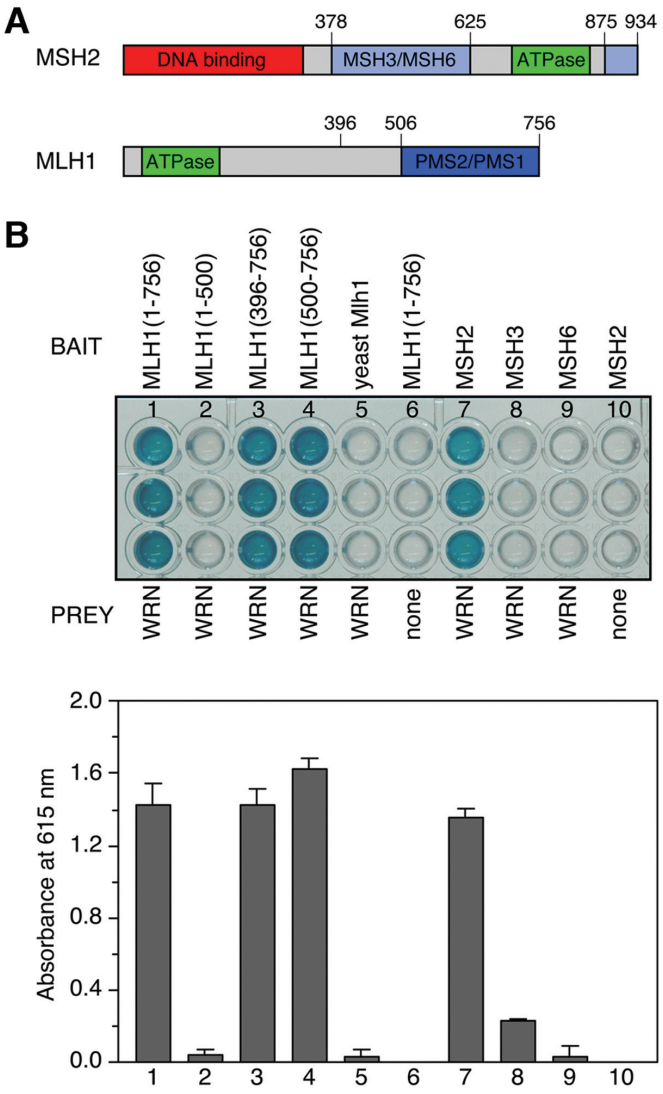

Figure 4. Interaction between WRN and MMR proteins in yeast two-hybrid system. (**A**) Domain organizations of the MSH2 and MLH1 proteins. The numbers refer to the amino acid sequence. (**B**) Quantitative yeast two-hybrid assay. The S. cerevisiae strain L40 harboring a pACT2 vector expressing the full-length WRN fused to the GAL4 activation domain was transformed with pBTM116 vectors encoding the indicated MMR proteins fused to LexA (MLH1 and its deletion derivatives, MSH3 and MSH6) or Gal4 (MSH2) DNA binding domains. Clones containing both plasmids were subjected to β-galactosidase assay on an ELISA micro-plate using 5-bromo-4-chloro-3-indolyl-β-D-galactopyranoside (X-gal) as a substrate. Top panel: An ELISA plate after a 30-min incubation at room temperature. Bottom panel: Graph showing absorbance at 615 nm measured in individual wells after 35 min, which is a measure of β-gal activity. The values represent the mean of three independent experiments.

DISCUSSION

Although WRN has been implicated in a number of DNA repair processes, the exact DNA transactions mediated by this helicase/exonuclease in the cell remain elusive. Here we show that WRN interacts physically with proteins that are involved in the initiation of MMR and the rejection of recombination between divergent sequences. Most importantly, our experiments revealed that MutSα and MutSβ can stimulate the helicase activity of WRN on forked DNA structures with a 3′-ss arm that resemble intermediates of single-strand annealing pathways of HR. In addition, we found that a single G/T mismatch located ahead of the fork junction increased the efficiency of the MutSα-dependent unwinding by WRN. These data are consistent with a model in which the MMR initiation factors prevent homeologous recombination by activating a DNA helicase for unwinding of recombination intermediates containing mismatches. This model was proposed earlier on the basis of results of *in vivo* heteroduplex rejection assays with yeast *msh2* and *sgs1* mutants (27,28). It is possible that MutSα and MutSβ bind to mismatches formed after pairing of sequences of imperfect homology and, following ATP binding, are converted into a DNA sliding clamp as proposed in the case of the MMR pathway (42). When the clamp encounters the junction between the heteroduplex and the non-homologous 3′-ss tail, it binds stably to it and recruits a DNA helicase to disrupt the joined DNA molecule. In agreement with this hypothesis, it has been demonstrated that yeast MutSβ specifically binds to forked DNA structures containing 3′- ssDNA making contacts with the sequences at the ds–ss junction (43). These studies also revealed that MutSβ holds the junction in an altered, perhaps more rigid, conformation (43). Such structural changes could facilitate the loading of the WRN helicase on the 3′- ssDNA at the junction, which is a prerequisite for duplex unwinding to occur. However, it should be noted that the MutSα-activated unwinding of a 3′-flap duplex by WRN displayed only a moderate dependence on mismatches. It is therefore possible that hereroduplex rejection *in vivo* involves some additional factors that ensure mismatch specificity of this transaction.

In our studies, we did not observe any significant modulation of WRN-mediated unwinding by MutLα, even in the presence of MutSα or MutSβ. In agreement with this finding, the yeast Mlh1 and Pms1 proteins have been shown to have only minor roles in the rejection of homeologous recombination relative to the contributions of Msh2 and Msh6 (27). Thus, it appears that the physical interaction between WRN and MutLα identified in this study has some other functional implication. Interestingly, MLH1 was shown to interact with various DNA repair factors including MRE11, BACH1, MBD4 and BLM (29,44–47). It is, therefore, possible that MLH1 plays a more general role in DNA repair processes.

A number of other functional implications for the observed interactions between WRN and the MMR factors can be discussed. Several lines of evidence suggest that WRN promotes replication of telomeric DNA by unwinding G-quadruplex structures that can readily form in G-rich telomeric DNA and impose a barrier for progression of DNA replication forks (9,48–50). Strikingly, human MutSα has been shown to bind efficiently to G-quadruplex DNA (51). Moreover, Msh2 deficiency in mice is associated with loss of telomeres and an elevated level of telomere end-to-end fusion, a phenotype similar to that manifested by WRN-deficient

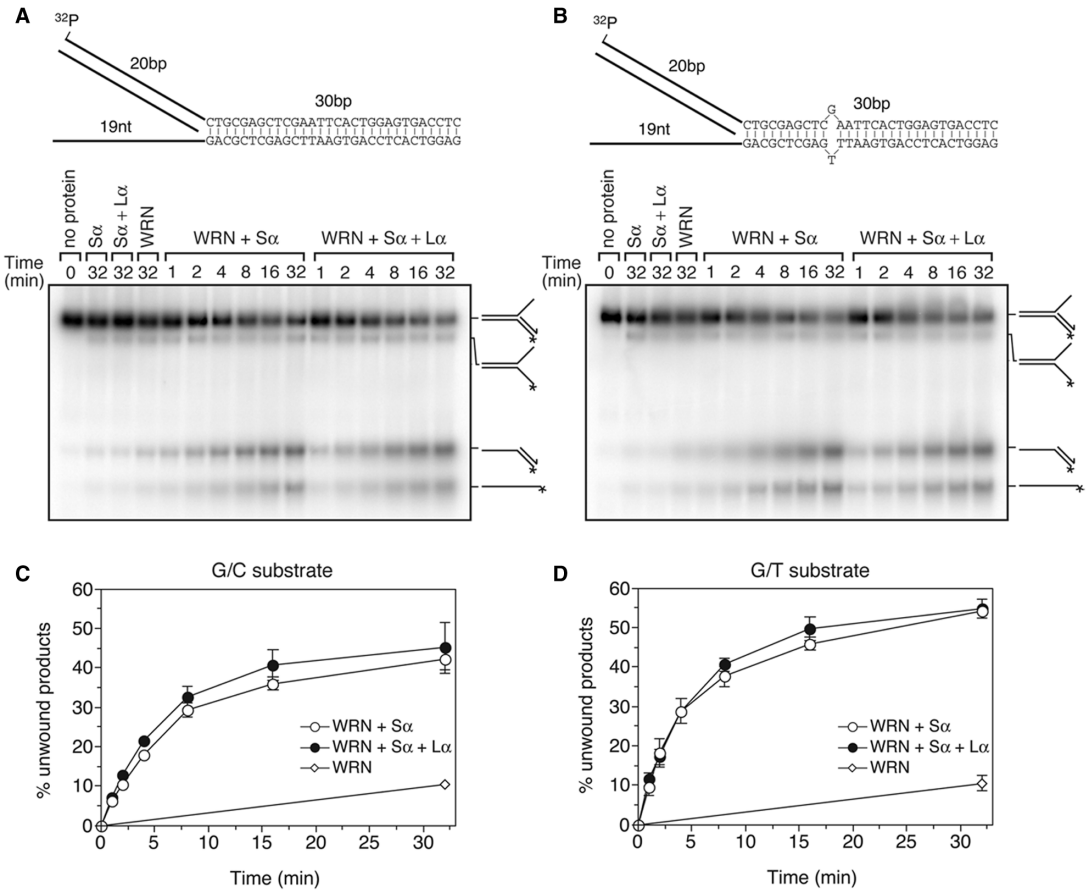

Figure 5. Kinetics of WRN-mediated unwinding of a 3′-flap DNA duplex in the presence of MutSα and MutLα. (**A**) Reactions with a homoduplex 3′ flap substrate. (**B**) Reactions with a 3′-flap duplex containing a G/T mismatch located 11 nucleotides ahead of the fork as indicated. (**C**) Quantification of the time course reactions in A. (**D**) Quantification of the time course reactions in B. All reactions contained 1 nM [^{32}P]DNA, 1 nM WRN and 8 nM MMR proteins as indicated. Aliquots at individual time points were analyzed by native PAGE followed by phosphorimaging and quantification as described in Materials and Methods section. Schemes of the substrate and the reaction products are shown on the right. The relative concentration of unwound products (3′-tailed duplex and free labeled oligonucleotide) is expressed as a percentage of total DNA.

cells (9,52). Thus, one can speculate that the MMR proteins can mediate recruitment of the WRN helicase to G-quadruplex structures formed at telomeres and hence facilitate their removal.

It has been shown that the human MutSβ and WRN are required along with PCNA, RPA and ERCC1-XPF for uncoupling of psoralen-induced inter-strand DNA crosslinks (ICLs) in cell-free extracts, suggesting a novel ICL-repair pathway in which MutSβ is essential for the recognition of ICLs, while the WRN helicase mediates unwinding of the DNA duplex adjacent to the lesion, which enables strand incision by ERCC1-XPF (53,54). Our finding that MutSβ physically interacts with WRN and stimulates its helicase activity brings further support for this model and suggests that MutSβ might recruit WRN to the ICL sites.

Earlier studies demonstrated that nuclear extracts from several fibroblastoid cell lines derived from WS patients were deficient in repair of base–base mismatches and insertion/deletion loops, suggesting that WRN could have a role in MMR (55). However, it is not certain that the MMR-deficiency of these extracts was caused solely by WRN deficiency because complementation experiments with recombinant WRN protein were not performed in this study. Moreover, in some cases, pairwise mixing of these extracts restored MMR proficiency, making the involvement of WRN in MMR rather questionable.

Recently, two other human RecQ homologs, namely RECQ1 and BLM, have been shown to interact physically and functionally with the MMR-initiation factors (29,31,47,56,57). As in the case of WRN, MutSα was found to stimulate RECQ1-mediated unwinding of a forked structure with a 3′-ss arm (56). In contrast, MutSα did not affect unwinding of forked DNA duplexes by BLM (31). Instead, MutSα was found to stimulate the ability of BLM to process Holliday junctions *in vitro* (57). Further studies will be needed to fully understand the molecular mechanisms by which the RecQ helicases and MMR factors work together to maintain genomic stability.

SUPPLEMENTARY DATA

Supplementary Data are available at NAR Online.

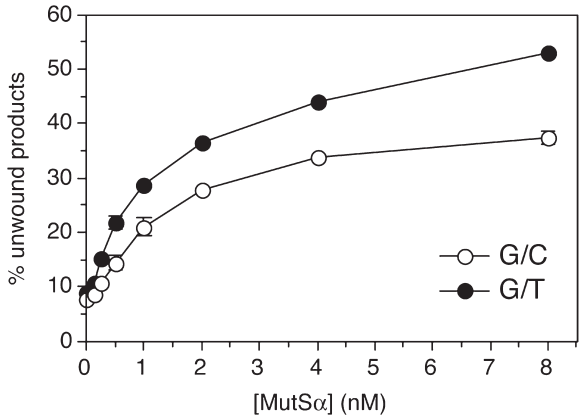

Figure 6. Helicase activity of WRN on 3′-flap duplexes with or without a G/T mismatch as a function of MutSα concentration. WRN and the DNA substrate were present at a concentration of 1 nM. The DNA substrates were the same as in Figure 5. Reactions were incubated for 30 min and analyzed by native PAGE followed by phosphorimaging as described in Materials and Methods section. The data points represent the mean of three independent experiments. The relative concentration of unwound products (3′-tailed duplex and free labeled oligonucleotide) is expressed as a percentage of total DNA.

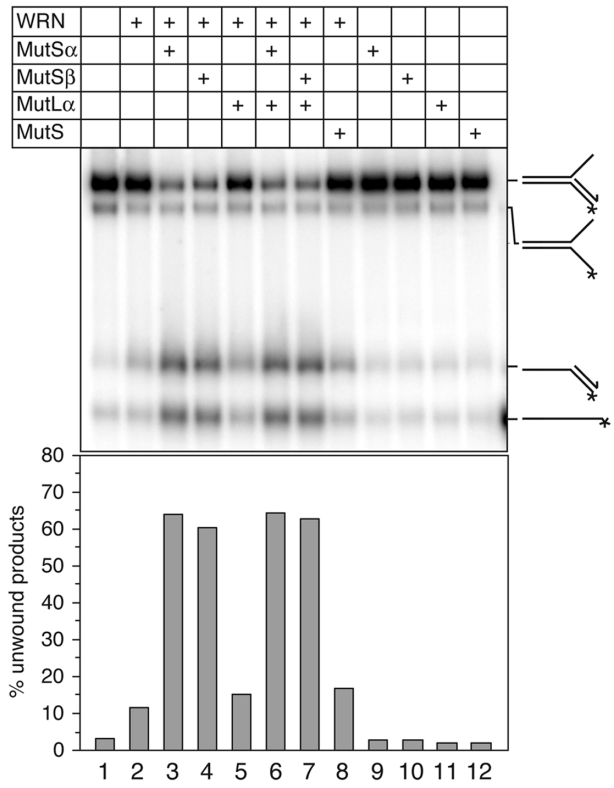

Figure 7. Effect of various MMR proteins on WRN-mediated unwinding of a 3′-flap DNA duplex. Helicase reactions contained 1 nM [^{32}P]DNA substrate and 2 nM WRN. The MMR proteins were present in a concentration of 8 nM as indicated. Reactions were incubated for 32 min and analyzed by native PAGE followed by phosphorimaging as described in Materials and Methods section (top panel). The relative concentration of unwound products (3′-tailed duplex and free labeled oligonucleotide) is expressed as a percentage of total DNA (bottom panel). Schemes of the substrate and the reaction products are shown on the right.

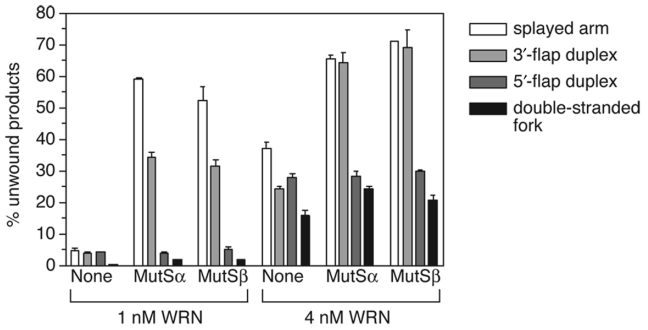

Figure 8. Stimulation of WRN-mediated unwinding of forked DNA structures by MutSα and MutSβ is dependent on the presence of 3′-single stranded DNA at the junction. Reactions with 1 nM splayed arm (white bars), 1 nM 3′-flap duplex (light gray bars), 1 nM 5′-flap duplex (dark gray bars) and 1 nM fully double-stranded fork duplex (black bars) contained 1 nM or 4 nM WRN and 8 nM MutSα or MutSβ as indicated. Reactions were incubated for 32 min and analyzed by native PAGE followed by phosphorimaging as described in Materials and Methods. The relative concentration of unwound products is expressed as a percentage of total DNA. The data points represent the mean of at least three independent experiments.

ACKNOWLEDGEMENTS

We thank Renjie Jiao for the construction of pACT2-WRN plasmid used in YTH assay, Peter Cejka for purified *E. coli* MutS protein and Lene Rasmussen for the plasmid pLJR105. We are also grateful to Josef Jiricny, Stefano Ferrari and David Lauterbach for comments on the manuscript. This work was supported by the Sassella and the Swiss National Science Foundations (Marie Heim-Vögtlin Grant Nr. PMPDA-102451 to N.S.). Funding to pay the Open Access publication charges for this article was provided by the Swiss National Science Foundation.

Conflict of interest statement. None declared.

REFERENCES

1. Martin,G.M. (1982) Syndromes of accelerated aging. *Natl. Cancer Inst. Monogr.*, **60**, 241–247.
2. Yu,C.E., Oshima,J., Fu,Y.H., Wijsman,E.M., Hisama,F., Alisch,R., Matthews,S., Nakura,J., Miki,T. *et al.* (1996) Positional cloning of the Werner's syndrome gene. *Science*, **272**, 258–262.
3. Gray,M.D., Shen,J.C., Kamath-Loeb,A.S., Blank,A., Sopher,B.L., Martin,G.M., Oshima,J. and Loeb,L.A. (1997) The Werner syndrome protein is a DNA helicase. *Nat. Genet.*, **17**, 100–103.
4. Huang,S., Li,B., Gray,M.D., Oshima,J., Mian,I.S. and Campisi,J. (1998) The premature ageing syndrome protein, WRN, is a 3′—>5′ exonuclease. *Nat. Genet.*, **20**, 114–116.
5. Kamath-Loeb,A.S., Shen,J.C., Loeb,L.A. and Fry,M. (1998) Werner syndrome protein. II. Characterization of the integral 3′ —> 5′ DNA exonuclease. *J. Biol. Chem.*, **273**, 34145–34150.
6. Fujiwara,Y., Higashikawa,T. and Tatsumi,M. (1977) A retarded rate of DNA replication and normal level of DNA repair in Werner's syndrome fibroblasts in culture. *J. Cell. Physiol.*, **92**, 365–374.
7. Rodriguez-Lopez,A.M., Jackson,D.A., Iborra,F. and Cox,L.S. (2002) Asymmetry of DNA replication fork progression in Werner's syndrome. *Aging Cell*, **1**, 30–39.
8. Saintigny,Y., Makienko,K., Swanson,C., Emond,M.J. and Monnat,R.J.Jr. (2002) Homologous recombination resolution defect in Werner syndrome. *Mol. Cell. Biol.*, **22**, 6971–6978.

9. Crabbe,L., Verdun,R.E., Haggblom,C.I. and Karlseder,J. (2004) Defective telomere lagging strand synthesis in cells lacking WRN helicase activity. *Science*, **306**, 1951–1953.
10. Fukuchi,K., Martin,G.M. and Monnat,R.J.Jr. (1989) Mutator phenotype of Werner syndrome is characterized by extensive deletions. *Proc. Natl Acad. Sci. USA*, **86**, 5893–5897.
11. Salk,D., Au,K., Hoehn,H. and Martin,G.M. (1985) Cytogenetic aspects of Werner syndrome. *Adv. Exp. Med. Biol.*, **190**, 541–546.
12. Salk,D., Au,K., Hoehn,H. and Martin,G.M. (1981) Cytogenetics of Werner's syndrome cultured skin fibroblasts: variegated translocation mosaicism. *Cytogenet. Cell. Genet.*, **30**, 92–107.
13. Crabbe,L., Jauch,A., Naeger,C.M., Holtgreve-Grez,H. and Karlseder,J. (2007) Telomere dysfunction as a cause of genomic instability in Werner syndrome. *Proc. Natl Acad. Sci. USA*, **104**, 2205–2210.
14. Poot,M., Gollahon,K.A., Emond,M.J., Silber,J.R. and Rabinovitch,P.S. (2002) Werner syndrome diploid fibroblasts are sensitive to 4-nitroquinoline-N-oxide and 8-methoxypsoralen: implications for the disease phenotype. *FASEB J.*, **16**, 757–758.
15. Poot,M., Yom,J.S., Whang,S.H., Kato,J.T., Gollahon,K.A. and Rabinovitch,P.S. (2001) Werner syndrome cells are sensitive to DNA cross-linking drugs. *FASEB J.*, **15**, 1224–1226.
16. Poot,M., Gollahon,K.A. and Rabinovitch,P.S. (1999) Werner syndrome lymphoblastoid cells are sensitive to camptothecin-induced apoptosis in S-phase. *Hum. Genet.*, **104**, 10–14.
17. Lan,L., Nakajima,S., Komatsu,K., Nussenzweig,A., Shimamoto,A., Oshima,J. and Yasui,A. (2005) Accumulation of Werner protein at DNA double-strand breaks in human cells. *J. Cell Sci.*, **118**, 4153–4162.
18. Cheng,W.H., von Kobbe,C., Opresko,P.L., Arthur,L.M., Komatsu,K., Seidman,M.M., Carney,J.P. and Bohr,V.A. (2004) Linkage between Werner syndrome protein and the Mre11 complex via Nbs1. *J. Biol. Chem.*, **279**, 21169–21176.
19. Cooper,M.P., Machwe,A., Orren,D.K., Brosh,R.M., Ramsden,D. and Bohr,V.A. (2000) Ku complex interacts with and stimulates the Werner protein. *Genes Dev.*, **14**, 907–912.
20. Baynton,K., Otterlei,M., Bjoras,M., von Kobbe,C., Bohr,V.A. and Seeberg,E. (2003) WRN interacts physically and functionally with the recombination mediator protein RAD52. *J. Biol. Chem.*, **278**, 36476–36486.
21. Karmakar,P., Piotrowski,J., Brosh,R.M.Jr, Sommers,J.A., Miller,S.P., Cheng,W.H., Snowden,C.M., Ramsden,D.A. and Bohr,V.A. (2002) Werner protein is a target of DNA-dependent protein kinase *in vivo* and *in vitro*, and its catalytic activities are regulated by phosphorylation. *J. Biol. Chem.*, **277**, 18291–18302.
22. Kunkel,T.A. and Erie,D.A. (2005) DNA mismatch repair. *Annu. Rev. Biochem.*, **74**, 681–710.
23. Jiricny,J. (2006) The multifaceted mismatch-repair system. *Nat. Rev. Mol. Cell. Biol.*, **7**, 335–346.
24. Jiricny,J. and Marra,G. (2003) DNA repair defects in colon cancer. *Curr. Opin. Genet. Dev.*, **13**, 61–69.
25. Kadyrov,F.A., Dzantiev,L., Constantin,N. and Modrich,P. (2006) Endonucleolytic function of MutLα in human mismatch repair. *Cell*, **126**, 297–308.
26. Myung,K., Datta,A., Chen,C. and Kolodner,R.D. (2001) SGS1, the *Saccharomyces cerevisiae* homologue of BLM and WRN, suppresses genome instability and homologous recombination. *Nat. Genet.*, **27**, 113–116.
27. Sugawara,N., Goldfarb,T., Studamire,B., Alani,E. and Haber,J.E. (2004) Heteroduplex rejection during single-strand annealing requires Sgs1 helicase and mismatch repair proteins Msh2 and Msh6 but not Pms1. *Proc. Natl Acad. Sci. USA*, **101**, 9315–9320.
28. Goldfarb,T. and Alani,E. (2005) Distinct roles for the *Saccharomyces cerevisiae* mismatch repair proteins in heteroduplex rejection, mismatch repair and nonhomologous tail removal. *Genetics*, **169**, 563–574.
29. Pedrazzi,G., Perrera,C., Blaser,H., Kuster,P., Marra,G., Davies,S.L., Ryu,G.H., Freire,R., Hickson,I.D. *et al.* (2001) Direct association of Bloom's syndrome gene product with the human mismatch repair protein MLH1. *Nucleic Acids Res.*, **29**, 4378–4386.
30. Rasmussen,L.J., Rasmussen,M., Lee,B., Rasmussen,A.K., Wilson,D.M.3rd, Nielsen,F.C. and Bisgaard,H.C. (2000) Identification of factors interacting with hMSH2 in the fetal liver utilizing the yeast two-hybrid system. *In vivo* interaction through the C-terminal domains of hEXO1 and hMSH2 and comparative expression analysis. *Mutat. Res.*, **460**, 41–52.
31. Pedrazzi,G., Bachrati,C.Z., Selak,N., Studer,I., Petkovic,M., Hickson,I.D., Jiricny,J. and Stagljar,I. (2003) The Bloom's syndrome helicase interacts directly with the human DNA mismatch repair protein hMSH6. *Biol Chem.*, **384**, 1155–1164.
32. Orren,D.K., Brosh,R.M.Jr, Nehlin,J.O., Machwe,A., Gray,M.D. and Bohr,V.A. (1999) Enzymatic and DNA binding properties of purified WRN protein: high affinity binding to single-stranded DNA but not to DNA damage induced by 4NQO. *Nucleic Acids Res.*, **27**, 3557–3566.
33. Palombo,F., Iaccarino,I., Nakajima,E., Ikejima,M., Shimada,T. and Jiricny,J. (1996) hMutSβ, a heterodimer of hMSH2 and hMSH3, binds to insertion/deletion loops in DNA. *Curr. Biol.*, **6**, 1181–1184.
34. Raschle,M., Marra,G., Nystrom-Lahti,M., Schar,P. and Jiricny,J. (1999) Identification of hMutLβ, a heterodimer of hMLH1 and hPMS1. *J. Biol. Chem.*, **274**, 32368–32375.
35. Lamers,M.H., Perrakis,A., Enzlin,J.H., Winterwerp,H.H., de Wind,N. and Sixma,T.K. (2000) The crystal structure of DNA mismatch repair protein MutS binding to a G x T mismatch. *Nature*, **407**, 711–717.
36. Brosh,R.M.Jr, von Kobbe,C., Sommers,J.A., Karmakar,P., Opresko,P.L., Piotrowski,J., Dianova,I., Dianov,G.L. and Bohr,V.A. (2001) Werner syndrome protein interacts with human flap endonuclease 1 and stimulates its cleavage activity. *EMBO J.*, **20**, 5791–5801.
37. Mockli,N. and Auerbach,D. (2004) Quantitative β-galactosidase assay suitable for high-throughput applications in the yeast two-hybrid system. *Biotechniques*, **36**, 872–876.
38. Janscak,P., Garcia,P.L., Hamburger,F., Makuta,Y., Shiraishi,K., Imai,Y., Ikeda,H. and Bickle,T.A. (2003) Caracterization and mutational analysis of the RecQ core of the bloom syndrome protein. *J. Mol. Biol.*, **330**, 29–42.
39. Lee,J.W., Harrigan,J., Opresko,P.L. and Bohr,V.A. (2005) Pathways and functions of the Werner syndrome protein. *Mech. Ageing Dev.*, **126**, 79–86.
40. Brosh,R.M.Jr, Waheed,J. and Sommers,J.A. (2002) Biochemical characterization of the DNA substrate specificity of Werner syndrome helicase. *J. Biol. Chem.*, **277**, 23236–23245.
41. Blackwell,L.J., Wang,S. and Modrich,P. (2001) DNA chain length dependence of formation and dynamics of hMutSα.hMutLα.heteroduplex complexes. *J. Biol. Chem.*, **276**, 33233–33240.
42. Gradia,S., Subramanian,D., Wilson,T., Acharya,S., Makhov,A., Griffith,J. and Fishel,R. (1999) hMSH2-hMSH6 forms a hydrolysis-independent sliding clamp on mismatched DNA. *Mol. Cell.*, **3**, 255–261.
43. Surtees,J.A. and Alani,E. (2006) Mismatch repair factor MSH2-MSH3 binds and alters the conformation of branched DNA structures predicted to form during genetic recombination. *J. Mol. Biol.*, **360**, 523–536.
44. Her,C., Vo,A.T. and Wu,X. (2002) Evidence for a direct association of hMRE11 with the human mismatch repair protein hMLH1. *DNA Repair (Amst.)*, **1**, 719–729.
45. Cannavo,E., Gerrits,B., Marra,G., Schlapbach,R. and Jiricny,J. (2007) Characterization of the interactome of the human MutL homologues MLH1, PMS1, and PMS2. *J. Biol. Chem.*, **282**, 2976–2986.
46. Bellacosa,A., Cicchillitti,L., Schepis,F., Riccio,A., Yeung,A.T., Matsumoto,Y., Golemis,E.A., Genuardi,M. and Neri,G. (1999) MED1, a novel human methyl-CpG-binding endonuclease, interacts with DNA mismatch repair protein MLH1. *Proc. Natl Acad. Sci. USA*, **96**, 3969–3974.
47. Langland,G., Kordich,J., Creaney,J., Goss,K.H., Lillard-Wetherell,K., Bebenek,K., Kunkel,T.A. and Groden,J. (2001) The Bloom's syndrome protein (BLM) interacts with MLH1 but is not required for DNA mismatch repair. *J. Biol. Chem.*, **276**, 30031–30035.
48. Kamath-Loeb,A.S., Loeb,L.A., Johansson,E., Burgers,P.M. and Fry,M. (2001) Interactions between the Werner syndrome helicase and DNA polymerase delta specifically facilitate copying of tetraplex and hairpin structures of the d(CGG)n trinucleotide repeat sequence. *J. Biol. Chem.*, **276**, 16439–16446.

49. Mohaghegh,P., Karow,J.K., Brosh,R.M.Jr, Bohr,V.A. and Hickson,I.D. (2001) The Bloom's and Werner's syndrome proteins are DNA structure-specific helicases. *Nucleic Acids Res.*, **29**, 2843–2849.
50. Vorlickova,M., Chladkova,J., Kejnovska,I., Fialova,M. and Kypr,J. (2005) Guanine tetraplex topology of human telomere DNA is governed by the number of (TTAGGG) repeats. *Nucleic Acids Res.*, **33**, 5851–5860.
51. Larson,E.D., Duquette,M.L., Cummings,W.J., Streiff,R.J. and Maizels,N. (2005) MutSα binds to and promotes synapsis of transcriptionally activated immunoglobulin switch regions. *Curr. Biol.*, **15**, 470–474.
52. Campbell,M.R., Wang,Y., Andrew,S.E. and Liu,Y. (2006) Msh2 deficiency leads to chromosomal abnormalities, centrosome amplification, and telomere capping defect. *Oncogene*, **25**, 2531–2536.
53. Zhang,N., Kaur,R., Lu,X., Shen,X., Li,L. and Legerski,R.J. (2005) The Pso4 mRNA splicing and DNA repair complex interacts with WRN for processing of DNA interstrand cross-links. *J. Biol. Chem.*, **280**, 40559–40567.
54. Zhang,N., Lu,X., Zhang,X., Peterson,C.A. and Legerski,R.J. (2002) hMutSbeta is required for the recognition and uncoupling of psoralen interstrand cross-links *in vitro*. *Mol. Cell. Biol.*, **22**, 2388–2397.
55. Bennett,S.E., Umar,A., Oshima,J., Monnat,R.J.Jr. and Kunkel,T.A. (1997) Mismatch repair in extracts of Werner syndrome cell lines. *Cancer Res.*, **57**, 2956–2960.
56. Doherty,K.M., Sharma,S., Uzdilla,L.A., Wilson,T.M., Cui,S., Vindigni,A. and Brosh,R.M.Jr. (2005) RECQ1 helicase interacts with human mismatch repair factors that regulate genetic recombination. *J. Biol. Chem.*, **280**, 28085–28094.
57. Yang,Q., Zhang,R., Wang,X.W., Linke,S.P., Sengupta,S., Hickson,I.D., Pedrazzi,G., Perrera,C., Stagljar,I. *et al.* (2004) The mismatch DNA repair heterodimer, hMSH2/6, regulates BLM helicase. *Oncogene*, **23**, 3749–3756.